

AMERICAN UNIVERSITY OF BEIRUT

CASCADED LIQUID DESICCANT SYSTEM FOR
HUMIDITY CONTROL IN SPACE CONDITIONED BY COOLED
MEMBRANE CEILING AND DISPLACEMENT VENTILATION

by
JINANE ABDALLAH CHARARA

A thesis
submitted in partial fulfillment of the requirements
for the degree of Master of Engineering
to the Department of Mechanical Engineering
of the Maroun Semaan Faculty of Engineering and Architecture
at the American University of Beirut

Beirut, Lebanon
August 2019

AMERICAN UNIVERSITY OF BEIRUT

THESIS/DISSERTATION FULL TITLE

by
JINANE ABDALLAH CHARARA

Approved by:


Prof. Kamel Abou Ghali, PhD, Professor
Department of Mechanical Engineering


Co- Advisor

Prof. Nesreen Ghaddar, PhD, Professor
Department of Mechanical Engineering


Co-Advisor

Prof. Ali Tehrani, PhD, Assistant Professor
Department of Chemical Engineering

Ali Tehrani 
Member of Committee

Date of thesis/dissertation defense: August 22, 2019

AMERICAN UNIVERSITY OF BEIRUT

THESIS, DISSERTATION, PROJECT RELEASE FORM

Student Name:

Charara

Jinane

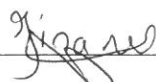
Aballah

Master's Thesis Master's Project Doctoral Dissertation

I authorize the American University of Beirut to: (a) reproduce hard or electronic copies of my thesis, dissertation, or project; (b) include such copies in the archives and digital repositories of the University; and (c) make freely available such copies to third parties for research or educational purposes.

I authorize the American University of Beirut, to: (a) reproduce hard or electronic copies of it; (b) include such copies in the archives and digital repositories of the University; and (c) make freely available such copies to third parties for research or educational purposes after:

- One ---- year from the date of submission of my thesis, dissertation, or project.**
- Two ---- years from the date of submission of my thesis, dissertation, or project.**
- Three ---- years from the date of submission of my thesis, dissertation, or project.**


Signature

August 27, 2019
Date

ACKNOWLEDGMENTS

First and foremost, I would like to express my deepest appreciation to my advisors, Professor Kamel Abou Ghali and Professor Nesreen Ghaddar for their conscientious guidance and encouragement during my Master's at the American University of Beirut. My sincere gratitude also goes to the member of my thesis committee: Dr. Ali Tehrani for his comments and suggestions, and to the faculty members and staff of the Mechanical Engineering Department for their help in the achievement of this work, especially, Ghassan, Dory, Roger, Hisham and Joseph.

I would also like to thank my fellow lab mates in the American University of Beirut: Racha Seblany, Safaa Khalil, Asmaa Jrad, Manar Younes, Hussein Daoud, Mariam Itani, Farah Mneimneh, Douaa Al Assaad, Elvire Katramiz Ghadir Awada, and Mohamad Hout and Nagham Ismail. I am grateful to them for their continuous love and support.

Last but not least, would also like to show deep gratitude and appreciation to my family members, my mother, father, sisters, brothers, my husband, my lovely son and my friends for their support throughout the past years.

AN ABSTRACT OF THE THESIS OF

Jinane Abdallah Charara for Master of Engineering
Major: Applied Energy

Title: Cascaded liquid desiccant system for humidity control in space conditioned by cooled membrane ceiling and displacement ventilation

Displacement ventilation combined with liquid desiccant membrane cooled ceiling is an efficient Heating, ventilation and Air conditioning system. However, it has limited performance in office spaces located in hot and humid climates and characterized by high internal loads due to the lack of ability to control the humidity. This study proposes a cascaded liquid desiccant system from the ceiling to be used in a liquid desiccant heat and mass exchanger in the supply duct to control the humidity in the space and reduce energy cost. To achieve this goal, a predictive integrated model for different components of the cascaded liquid desiccant system is developed to predict the comfort level and the air quality inside the space as well as the energy consumption of the system. The model was validated experimentally in a climatic chamber.

The validated integrated model was applied to a case study to assess the effectiveness of the system in the hot and humid climate of Beirut. Two configurations of the liquid desiccant membrane cooled ceiling and mass exchanger were simulated and found to provide acceptable humidity for comfort in the occupied zone of the space. However, the cascaded system cooling and heating energy during the cooling season were found lower by 21.25% and 16.23% respectively in August when compared to a liquid desiccant membrane cooled ceiling, displacement ventilation and membrane exchanger system with different configuration. The cooling and heating energies were also lower in the cascaded system compared to a liquid desiccant membrane cooled ceiling, displacement ventilation and conventional dehumidification method.

CONTENTS

ACKNOWLEDGMENTS	v
ABSTRACT	vi
ILLUSTRATIONS	viii
TABLES	ix
LIST OF ABBREVIATIONS	x
chapter	
I. CASCADED COOLED LIQUID DESICCANT MEMBRANE CEILING WITH DISPALCEMENT VENTILATION AND MEMBRANE EXCHANGER	1
A. Introduction.....	1
B. System Description	5
II. MATERIALS AND METHODS	9
A. Mathematical formulation.....	10
1. The space model	10
2. Liquid desiccant membrane cooled ceiling	12
3. Heat and Moisture Membrane Exchanger	14
4. Regeneration strategy	17
5. Integration of space and system models and numerical simulation method...	19
B. Experimental Methodology	22
1. Experimental set up	22
2. Experimental protocol.....	24
III. RESULTS AND DISCUSSION	27
A. Experimental validation	27
B. Applicability of the humidity control strategy to a case study	29
1. Description of the case study	30
2. Performance of the liquid desiccant membrane cooled ceiling combined with displacement ventilation system for the different humidity control strategies	32
3. Energy Analysis	41
C. Conclusions.....	44
BIBLIOGRAPHY	45

ILLUSTRATIONS

Figure	Page
1: The proposed cascaded system for indoor air conditioning	7
2: Illustration of a room conditioned with a DV system	11
3: Illustration of the mass and energy transfer at the ceiling level	14
4: Illustration of the parameters of the flows in the membrane exchanger	15
5: Sequence of numerical solution flow chart	21
6: (a) Illustration of the experimental setup and (b) Photo of the experimental setup	23
7: Internal sensible and latent loads' distributions in the considered office for a typical summer day	31
8: Relative Humidity in the occupied zone of the considered indoor space for the LDMC-C/DV base case.....	35
9: Relative Humidity in the occupied zone of the considered indoor space for the LDMC-C/DV cascaded system.	38
10: Relative Humidity in the occupied zone of the considered indoor space for the LDMC-C/DV and membrane exchanger with separate feedlines.....	41
11: Monthly cooling energy consumption of the different LDMC-C/DV configurations for humidity control	43
12: Monthly heating energy consumption of the different LDMC-C/DV configurations for humidity control	44

LIST OF TABLES

Table	Page
1: Different inlet conitions for the three cases.....	26
2: Experimental and simulation results for different cases.....	28
3: Ambient Temperature and Relative humidity in four typical days during the summer season in Beirut, Lebanon	31
4: Results of base LDMC-C/DV case without dehumidification at DV supply.....	33
5: Results of LDMC-C/DV with membrane exchanger cascaded system.....	36
6: Results of LDMC-C/DV in the separate feed lines configuration.....	39

LIST OF ABBREVIATIONS

<i>A</i>	cross section area (m^2)
<i>C</i>	concentration of liquid desiccant ($\text{kg H}_2\text{O} / \text{kg dry desiccant}$)
<i>C-C</i>	cooled ceiling
<i>C_p</i>	specific heat ($\text{J/kg}\cdot\text{K}$)
<i>DV</i>	displacement Ventilation
<i>G</i>	Superficial air velocity ($1/\text{m}\cdot\text{s}$)
<i>H</i>	Enthalpy (kJ/kg)
<i>HVAC</i>	Heating ,Ventilation and Air Conditioning
<i>h_{fg}</i>	latent heat of vaporization of the water (kJ/kg)
<i>h_T</i>	convective heat transfer coefficient ($\text{W}/\text{m}^2\cdot\text{K}$)
<i>IAQ</i>	Indoor Air Quality
<i>K</i>	thermal conductance per unit length
<i>k</i>	thermal conductivity ($\text{W}/\text{m}\cdot\text{K}$)
<i>L</i>	superficial solution velocity ($1/\text{m}\cdot\text{s}$)
<i>LDMC-C</i>	Liquid Desiccant Membrane Cooled Ceiling
<i>m</i>	mass flow rate (kg/s)
<i>N</i>	number of heat sources
<i>PMV</i>	Predicted Mean Vote
<i>Q</i>	upward volumetric flow rate (m^3/s)
<i>q</i>	rate of heat transfer (W)

RH	Relative humidity (%)
T	temperature (°C)
U_c	overall heat transfer coefficient per unit length
U_m	overall mass transfer coefficient per unit length
W	humidity ratio (kg _{H2O} /kg _{dry air})
w	width (m)
x	distance from the inlet of the membrane (m)
ρ	density (kg/m ³)

Subscripts

a	room air
air	air stream
av	average
BDL	Air boundary layer
c	Ceiling
e	exchanger
k	index representing the orientation of wall
m	membrane
s	supply
sol	Solution stream
w	wall

CHAPTER I

CASCADED COOLED LIQUID DESICCANT MEMBRANE CEILING WITH DISPALCEMENT VENTILATION AND MEMBRANE EXCHANGER

A. Introduction

Nowadays people spend most of their time in indoor spaces (EPA, 1989). Hence their productivity and health are highly related to their satisfaction with the indoor thermal environment (thermal comfort) as well as the breathable air quality. For this reason, heating ventilation and air conditioning systems (HVAC) are implemented in today's buildings (Vesely an Zeiler, 2015). Thermal comfort is commonly achieved by assuring an adequate level of air room temperature while indoor air quality (IAQ) is affected by the concentration of contaminants in the space (Al Assaad et al., 2017). These two criteria are provided by conventional HVAC systems through continuous mixing of a significant percentage of cold fresh supply air with the warm contaminated air inside the space which requires high energy consumption (Itani et al., 2015). Hence, the design of energy-efficient HVAC systems is necessary (Chua at al., 2012).

One of the efficient ventilation systems is the combined cooled ceiling (CC) and displacement ventilation (DV) system (Ghaddar et al., 2010). DV provides a good breathable environment in the occupied zone through a continuous supply of 100% fresh air near the floor level (Yuan et al., 1998). Due to vertically rising air, the DV established a stratified airflow in the space and divided it into two zones: a lower cool and clean occupied zone, and an upper contaminated zone located above the breathing

level of occupants (Mossolly et al., 2008). The cooled ceiling assured the thermal comfort of occupants by radiative and convective heat removal (Hao et al., 2007). The combined system provides healthy and thermally comfortable conditions inside the space. However, the combined CC/DV system has some drawbacks. Actually, in cases where the air temperature next to the ceiling drops below the dew point, condensation may occur at the ceiling level contributing to potential IAQ hazards and mold growth (Younis et al., 2015). These concerns constrained the temperature of radiant ceiling, typically cooled by chilled water, to be higher than the dew point temperature of the air near the ceiling (Yin et al., 2014), which limited the capacity of such system in removing high space loads (Keblawi et al., 2011). To overcome this limitation, researchers considered replacing the cooled ceiling with a semi-permeable membrane ceiling cooled by liquid desiccant flow (Fanchoux et al., 2009). This system relied on the high concentration desiccant solution to absorb water vapor through the semi-permeable membrane; thus allowing the cooled ceiling to operate at lower temperatures. Accordingly, the system was reported to achieve effective radiant cooling without the risk of condensation, extending the overall heat load removal range of the CC/DV system (Hout et al., 2017).

The liquid desiccant membrane cooled ceiling combined with displacement ventilation system LDMC-C/DV was the core of several studies. Keniar et al. (2015) showed that the liquid desiccant flowing in vertical membrane tubes reduced the humidity of the air stream near the tubes. Muslamni et al. (2016) simulated the energy performance of an LDMC-C/DV system and showed about half of the total energy can be saved when using their proposed system compared to a conventional CC/DV

system. Nevertheless, the work of Muslmani et al. (2016) did not take into consideration the effect of moisture and heat extraction on the air flow adjacent to the ceiling level which created a dehumidified cold air boundary layer zone with different properties from the upper contaminated recirculation zone. Hence, their model was improved by Hout et al. (2017) to take into consideration the transfer of heat and moisture in the zone near the ceiling. Furthermore, Hout et al. (2017) reported the appropriate air flow rates and temperatures of the desiccant solution that would not cause condensation on the membrane ceiling for different DV supply air and liquid desiccant conditions.

Even though the radiant membrane ceiling was able to operate at lower temperatures, the system had a drawback. Results in the previous studies indicated that the *LDMC-C/DV* system did not provide any regulation of the humidity level especially in the lower occupied zone. Hout et al. (2017) reported that the relative humidity (RH) of the indoor air was relatively high in the presence of high internal moisture generation and high outdoor humidity cases. Hence, they recommended feasible conditions for operating the system such that comfort is maintained in the occupied zone and condensation would not occur (Hout et al., 2017). This resulted in small feasible region of operation in warm/hot humid climates. Although the increase of cooling capacity due to the presence of the membrane system was desirable for thermal comfort enhancement, the lack of humidity control in the lower occupied zone would adversely affect the comfort level and IAQ in the occupied zone. Seblany et al. (2018) proposed a humidity control method for the *LDMC-C/DV* system based on mixing the DV supply air with a fraction of the cold dehumidified exhaust air. This fraction respected the

maximum allowable CO₂ concentration value. However, it did not retain acceptable IAQ in case of high internal generation of contaminants and odors. Moreover, high internal moisture generation cases required higher exhaust air fraction which can deteriorate IAQ also in terms of CO₂ level.

Therefore, the high humidity levels in a *LDMC-C/DV* system established the need for a more effective humidity control strategy based on the dehumidification of *DV* supply air. A feasible strategy is to take advantage of cooled liquid desiccant which can also reduce the sensible heat of the air at supply while still using 100% fresh air for the *DV* supply; thus keeping the high indoor air quality feature of the *DV* system intact. The transfer of heat and moisture at *DV* supply can be achieved by using a membrane exchanger that eliminates the problem of desiccant droplet carryover which was a major concern in direct-contact dehumidifiers/regenerators (Abdel-Salam and Simonson, 2015). By that, the air-conditioning system is comprised of two air conditioning subsystems that need to be supplied by liquid desiccant; the *DV* equipped with membrane heat and mass exchanger outside the space, and the indoor membrane ceiling system. Therefore, one of the options that can be energy efficient is to direct the desiccant exiting from the membrane ceiling system to the membrane exchanger (Charara et al., 2018). Since the *LDMC-C/DV* allowed lower inlet solution temperatures, lower outlet solution temperatures are expected compared to conventional *CC/DV* systems. Thus, the desiccant solution at the outlet of the ceiling still has the capacity to cool and also to extract moisture from *DV* fresh air supply before it enters the space (Keniar et al., 2015). Consequently, directing the solution that leaves the membrane ceiling into the membrane exchanger is worth considering. To the author'

knowledge, the previously studied *LDMC-C/DV* systems did not provide any energy-efficient and safe humidity control strategy. Therefore, the proposed cascaded system would be unique in offering an energy efficient and safe humidity control method while having an indoor and an outdoor connected units; the indoor unit is the cooled liquid desiccant membrane ceiling system for enhancing sensible cooling in the space and the outdoor unit is the mass and heat exchanger for dehumidifying *DV* supply fresh air.

The aim of this work is to study the performance of a cascaded liquid desiccant system in which the cool and strong desiccant solution flows first into the membrane ceiling system in the space, and then into the heat and moisture *DV* exchanger in the *DV* supply duct. To predict the performance of the system, an integrated mathematical model is developed of all involved sub-systems. These sub-systems are: the indoor membrane ceiling, the *DV* system, the liquid desiccant membrane exchanger and the regenerator. The cascaded system is validated experimentally by comparing predicted and experimentally-measured temperatures and concentrations in air and desiccant flows. The energy efficiency of the cascaded system is assessed by comparing the thermal energy needs of the cascaded system with the energy consumed by other *LDMC-C/DV* configurations with different humidity control strategies.

B. System Description

The cascaded liquid desiccant system consists of two air conditioning subsystems: a ceiling desiccant membrane system to provide radiant cooling and a controlled displacement ventilation system. **Fig. 1** illustrates the indoor space

conditioned by the cascaded system and shows the flows of the desiccant solution and the air. The cooled solution is first introduced to the ceiling at (1) to extract heat and moisture from the air boundary layer at the vicinity of the ceiling. The exiting solution at (2) is sent to the compact heat and moisture exchanger in order to reduce the sensible and latent load of the DV supply air. A semi-permeable membrane achieves the transfer of heat and moisture in the two membrane subsystems. The solution leaving the membrane heat and moisture exchanger at (3) is preheated by through a liquid-liquid heat exchanger at (4). Then, the solution is further heated in the heating section at (5) followed by the regeneration at (6) where the concentration of the desiccant solution is restored back to the initial value. The solution is subjected to sensible cooling at (7) in order to set its inlet temperature to the desired value before entering the indoor space.

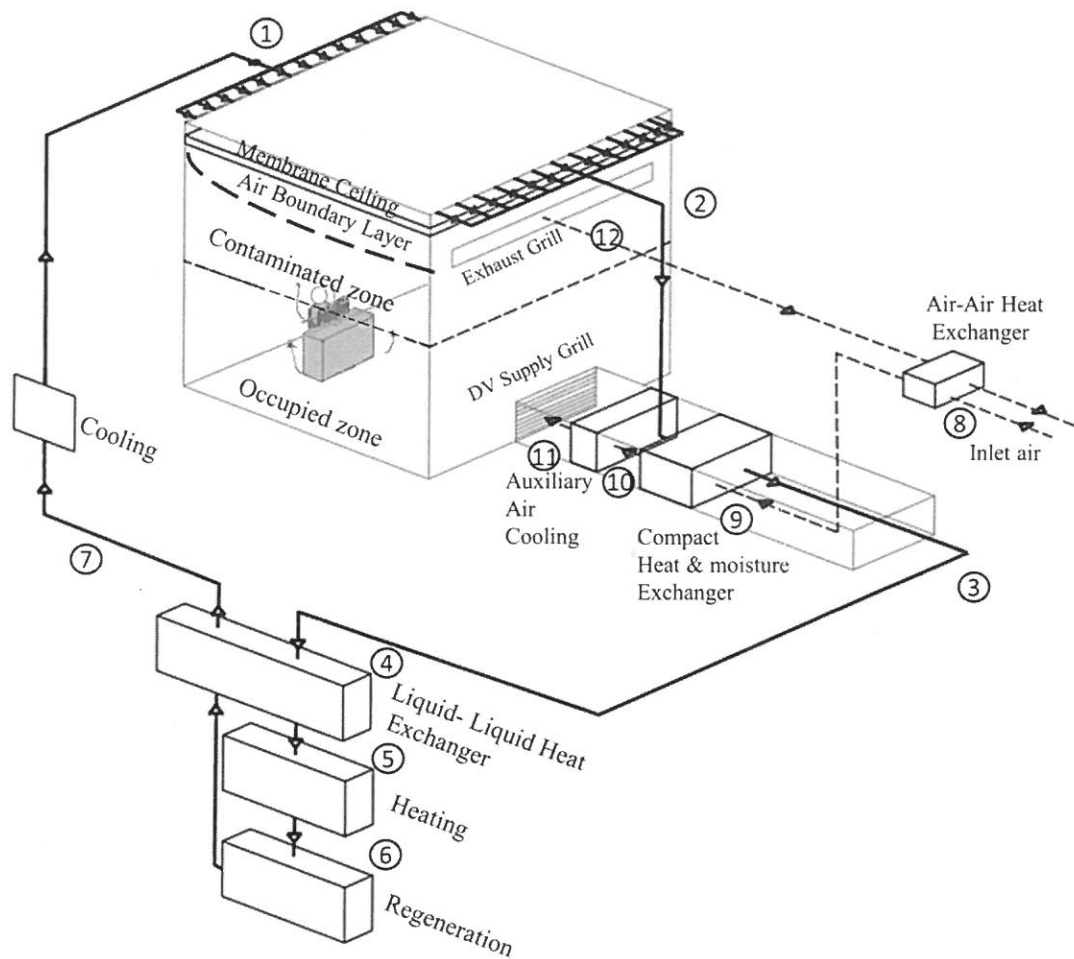


Fig. 1: The proposed cascaded system for indoor air conditioning

As for the flow of air through the system, it is first pre-cooled at (8) with the cold air leaving the exhaust grill at (12) via an Air-Air Heat Exchanger. The precooled air enters the membrane exchanger at (9) in order to be supplied to the indoor space through a *DV* supply grill at (11). If the cooling capacity of the membrane exchanger is not sufficient to achieve the needed temperature level of the supplied air, the auxiliary sensible cooling coil at (10) is used. The cold and fresh air supplied to the room is warmed by the heat sources in the space such as the occupants, lights, and electrical equipment. This establishes a natural upward convective flow that displaces the warm and

contaminated air vertically to be withdrawn through the exhaust grill at (12). The lower occupied zone and the higher contaminated zone are separated virtually by the stratification height, which is the level where the mass flow rate of air entrained by the buoyancy plumes becomes equivalent to the supply flow rate.

CHAPTER II

MATERIALS AND METHODS

The performance of the cascaded liquid desiccant ceiling membrane and mass exchanger system was studied by mathematical modeling to evaluate the effectiveness of humidity control method as well as associated energy consumption. Mathematical models were developed based on mass and energy balances of the air and desiccant flows for the following sub-systems: i) the DV-conditioned space, ii) liquid desiccant membrane cooled ceiling model, iii) the heat and moisture exchanger model, and iv) the regenerator model. The four models were integrated to predict the conditions of the air in the occupied zone which were used to evaluate the level of thermal comfort and IAQ. Moreover, the energy usage of the cascaded system was also determined using the integrated model while taking into consideration the cooling and heating needs of the various sub-systems.

The integrated model predictions of air and desiccant flow conditions were validated experimentally in a climatic chamber equipped with a *LDMC-C/DV* system and coupled with a membrane heat and mass exchanger. Then, the integrated model was applied to a case study where its energy performance in the hot and humid climate of Beirut was compared with systems using different humidity control strategies.

A. Mathematical formulation

Since the membrane exchanger in the cascaded system uses the conditions of the liquid desiccant exiting from the ceiling to provide the desired DV supply air temperature and humidity content. Furthermore, the regenerator that absorbs heat increases the concentration of the solution exiting from the membrane exchanger and restores it back to its value at the inlet of the ceiling. Consequently, the four sub-models are integrated to predict the overall system performance. The sub-models (Indoor DV space model, liquid desiccant membrane cooled ceiling model, heat and moisture exchanger model, and regenerator model) are presented in this section followed by their integration and numerical solution method.

1. *The space model*

The DV system supplies cold and fresh air to the space near the floor (Makhoul et al., 2013). When the supplied air encounters an internal heat source (e.g., occupants, electrical equipment, walls etc.), rising thermal plumes are formed, creating a natural upward convective flow due to the difference in density between the hot and the cold air (Al Assaad et al., 2018). This rising air drives the contaminants from the occupied zone to be exhausted at ceiling level as shown in **Fig. 2**. Accordingly, a mathematical model is needed to predict the temperature and humidity distributions in the space for given internal load and external conditions. Thus, the simplified space thermal model of (Ayoub et al., 2016) was adopted. The model input parameters are the outdoor weather conditions, the supply air temperature, relative humidity and flow rate,

internal load resulting from the lumped source, the ceiling temperature, the space envelope layering and physical characteristics, and the space dimensions.

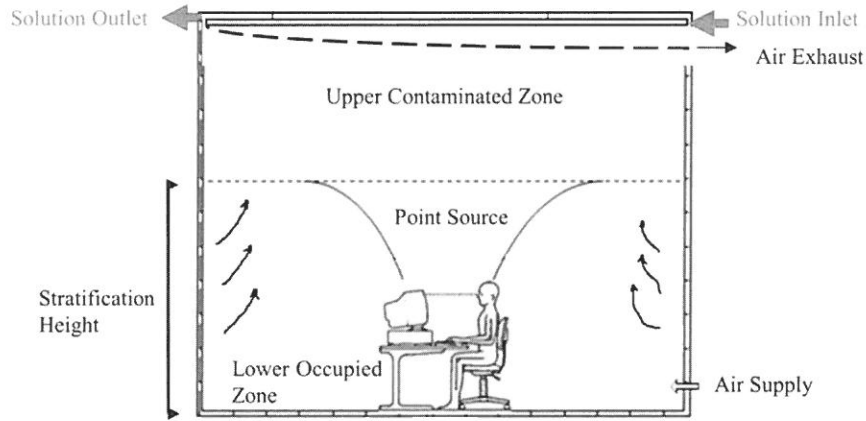


Fig. 2: Illustration of a room conditioned with a DV system

As shown in **Fig. 2**, the space is divided into two zones; a lower fresh occupied zone and an upper contaminated zone separated by the stratification height which is the level at which the flow rate of the air entrained by the plumes equals the supply flow rate as represented in the following equation (Schiavon et al., 2006).

$$\dot{m}_s = \rho_a N Q_{plume} + \rho_a \sum_{k=1}^n Q_{w,k} \quad (1)$$

where \dot{m}_s is the supply air mass flow rate, ρ_a is the density of the air, N is the number of point sources inside the room, and n is the number of walls. $Q_{w,k}$ is the volumetric flow rate entrained by each wall, and Q_{plume} is the flow entrained by each plume at a specific height z having a specific average temperature T_{av} (Mund, 1996). The parameters $Q_{w,k}$ and Q_{plume} are determined using Eq. (2), Eq. (3), Eq. (4) and Eq. (5) where M_w is the mass flow rate of air entrained by each wall, q is the rate of heat transfer and T_w is the temperature of the wall (Jaluria, 1994).

$$M_w = 0.00287 \times \rho_a \times (T_w - T_{av})^{0.25} \times z^{0.75} \times W \quad (2)$$

$$Q_{\text{plume}} = 0.00238 \times q^{3/4} \left(\frac{dT_{av}}{dz} \right)^{-5/8} \times \delta \quad (3)$$

With

$$\delta = 0.004 + 0.039\varphi + 0.38\varphi^2 - 0.062\varphi^3 \quad (4)$$

$$\varphi = 2.86 \times q^{-1/4} \left(\frac{dT_{av}}{dz} \right)^{3/8} \times z \quad (5)$$

2. *Liquid desiccant membrane cooled ceiling*

In order to compute conditions at ceiling level, a predictive mathematical model for the membrane cooled ceiling is needed. The model must take into consideration the transfer of moisture through the membrane which results in the formation of an adjacent air boundary layer that has different temperature and moisture conditions than the upper contaminated zone as shown in **Fig. 3**. For that reason, the model of Hout et al. (2017) was adopted. The model predicted the conditions of the solution side and the conditions of the air boundary layer using the temperature and humidity of the upper zone, the mass of water vapor entrained to the ceiling and the condition of solution at the inlet. Steady-state conditions were assumed while neglecting axial conduction and vapor diffusion. In addition, the temperature, velocity, and mass boundary layer thicknesses of air were considered equal while energy and mass storage in the boundary layer and the ceiling desiccant panel were neglected. Applying these

assumptions, energy balance equations for the desiccant and air sides were given respectively by Eq. (6) and Eq. (7).

$$\underbrace{-\dot{m}_{sol} \frac{\partial(C_{p,sol}T_{sol})}{\partial x}}_{\text{Net convective heat flow}} + \underbrace{U_{c,c}w_{m,c}(T_{BDL} - T_{sol})}_{\text{sensible heat transfer between air boundary layer and solution}} + \underbrace{U_{m,c} \rho_{air} h_{fg} w_{m,c} (W_{BDL} - W_{sol})}_{\text{heat released due to moisture exchanger}} = 0 \quad (6)$$

$$\underbrace{-\dot{m}_{BDL} C_{p,air} \frac{\partial(C_{p,air}T_{BDL})}{\partial x}}_{\text{Net convective heat flow}} + \underbrace{U_{c,c} w_{m,c} (T_{sol} - T_{BDL})}_{\text{Sensible heat transfer between air boundary layer and solution}} + \underbrace{U_{m,c} w_{m,c} \rho_{air} h_{fg} (W_{sol} - W_{BDL})}_{\text{Latent energy removed due to moisture exchange}} = 0 \quad (7)$$

$$+ \underbrace{\dot{m}_{entrained} C_{p,air} T_a}_{\text{Convective energy flow of the air entrained from the upper zone}} = 0$$

The solution mass flow rate, specific heat, temperature and equivalent humidity ratio are represented by \dot{m}_{sol} (kg/s), $C_{p,sol}$ (J/kg K), T_{sol} (K), W_{sol} (kg of H₂O/kg of dry air) respectively, while \dot{m}_{BDL} (kg/s), T_{BDL} (K), W_{BDL} (kg of H₂O/kg of dry air) and $C_{p,air}$ (J/kg K), are the mass flow rate, temperature, humidity ratio and specific heat in the air boundary layer respectively. $w_{m,c}$ is the width of the membrane at the ceiling, h_{fg} (J/kg) is the latent heat of vaporization of water, $\dot{m}_{entrained}$ is the mass flow rate of air displaced from the upper zone to the boundary layer zone and T_a (K) is the temperature room air;. The heat transfer coefficient $U_{c,c}$ and the mass transfer coefficients $U_{m,c}$ of the ceiling membrane were calculated using the equations of Hout et al. (2017).

The mass transfer equations for the desiccant and air sides were given respectively by Eq. (8) and Eq. (9) where C_{sol} (kg of H₂O/kg of dry desiccant) is the concentration of the solution and W_a is the air humidity in the room.

$$\underbrace{-\dot{m}_{sol} \frac{\partial(C_{sol})}{\partial x}}_{\text{Net convective moisture flow}} + \underbrace{U_{m,c} \rho_{air} W_{m,c} (W_{BDL} - W_{sol})}_{\text{Moisture transferred to the solution}} = 0 \quad (8)$$

$$\underbrace{-\dot{m}_{BDL} \frac{\partial(W_{BDL})}{\partial x}}_{\text{Net convective moisture flow}} + \underbrace{U_{m,c} \rho_{air} W_{m,c} (W_{sol} - W_{BDL})}_{\text{Moisture transferred to the solution}} + \underbrace{\dot{m}_{entrained} W_a}_{\text{Convective moisture flow of the air entrained from the room to the boundary layer}} = 0 \quad (9)$$

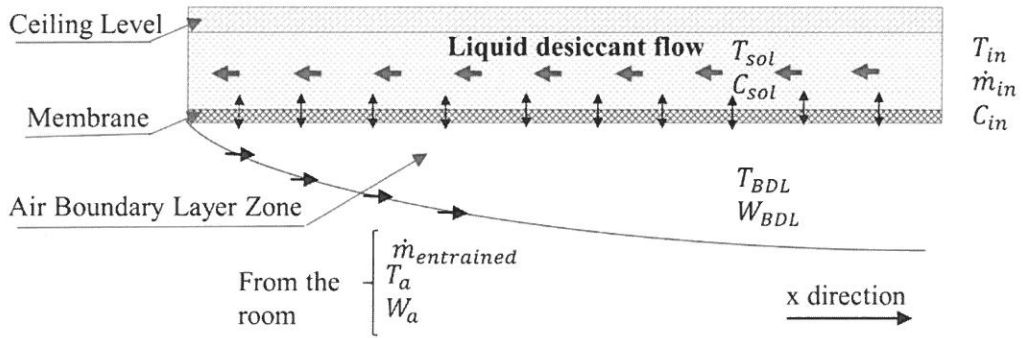


Fig. 3: Illustration of the mass and energy transfer at the ceiling level

3. Heat and Moisture Membrane Exchanger

A membrane heat and moisture exchanger is used to cool and dehumidify the supply air. The presence of the membrane allows the transfer of sensible and latent energy without any carryover of liquid desiccant (Zhang, 2008). One of the well-documented literature heat and moisture membrane exchanger model is the parallel plate configuration due to its simple design and low probability of leakage (Grossman, 2004). In a parallel plate membrane exchanger, the two flows of liquid desiccant and air are separated by a semi-permeable membrane allowing the transfer of water vapor (Abel-Salam et al., 2013). In this study, the model developed by Mustapha et al. (2017)

was used to represent the steady-state performance of the exchanger. The model predicted the humidity ratio and the temperature of the air leaving the exchanger in addition to the humidity and temperature of the solution in the liquid desiccant passages. Their model assumed that the flow was fully developed and that the latent heat of the water vapor exchanged was released only into the desiccant side. Moreover, the model assumed that each side of the membrane had a temperature that differed from the temperature of the adjacent flow, which caused heat transfer between the two sides of the membrane.

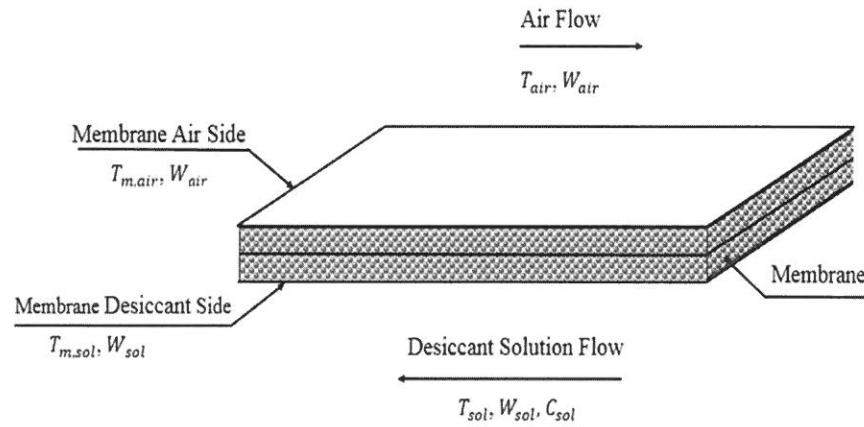


Fig. 4: Illustration of the parameters of the flows in the membrane exchanger

By applying the assumptions stated beforehand, the 1-D steady-state heat and moisture conservation in the air stream were represented in Eq. (5) and Eq. (6) respectively:

$$\underbrace{\dot{m}_{air} C_{p,air} \frac{dT_{air}}{dx}}_{\text{convective heat flow}} + \underbrace{h_{T,air} W_{m,e} (T_{air} - T_{m,air})}_{\text{heat transferred from the air to membrane air side}} = 0 \quad (10)$$

$$\underbrace{\dot{m}_{air} \frac{dW_{air}}{dx}}_{\text{convective moisture flow}} + \underbrace{U_{m,e} w_{m,e} (W_{air} - W_{sol})}_{\text{moisture transferred from the air to the solution}} = 0 \quad (11)$$

where \dot{m}_{air} (kg/s), T_{air} (K), W_{air} (kg of H₂O/kg of dry air) and $C_{p,air}$ (kJ/kg K) are the mass flow rate, temperature of the dry air, and humidity ratio and specific heat capacity of the air stream respectively, W_{sol} is the solution equivalent humidity ratio, $T_{m,air}$ (K) is the temperature of the membrane side that is adjacent to the air flow, x is the direction of air flow and $w_{m,e}$ (m) is the width of the membrane in the exchanger. $U_{m,e}$ (Kg/m²·s) is the overall mass exchange coefficient between the air and the solution and $h_{T,air}$ (kW/m² K) is the convective heat exchange coefficient between the membrane and the air stream.

Similarly, the heat and moisture conservation in the desiccant stream respectively are given by

$$\underbrace{\dot{m}_{sol} C_{p,sol} \frac{dT_{sol}}{dx}}_{\text{convective heat flow}} + \underbrace{h_{T,sol} w_{m,e} (T_{sol} - T_{m,sol})}_{\text{sensible heat transfer between the solution and the membrane solution side}} + \underbrace{U_{m,e} h_{fg} w_{m,e} (W_{sol} - W_{air})}_{\text{latent heat added due to transfer of moisture into the solution}} = 0 \quad (12)$$

$$\underbrace{\dot{m}_{sol} \frac{\partial C_{sol}}{\partial x}}_{\text{convective mass flow}} - \underbrace{U_{m,e} w_{m,e} (W_{air} - W_{sol})}_{\text{moisture transfer to the solution}} = 0 \quad (13)$$

where \dot{m}_{sol} (kg/s), T_{sol} (K), $C_{p,sol}$ (kJ/kg K) and C_{sol} (kg of H₂O/ kg of dry desiccant) are the mass flow rate, temperature of the dry solution, and humidity ratio, specific heat capacity and concentration of the solution stream, respectively. $h_{T,sol}$ (kW/m² K) is the convective heat exchange coefficient between the membrane and the desiccant stream.

Since the mass transfer across the membrane is assumed instantaneous and does not affect its energy balance, the energy conservation equations for the air side and the liquid desiccant side of the membrane are respectively given by

$$\begin{aligned}
 & \underbrace{k_m \frac{A_m}{2} \frac{\partial^2 T_{m,air}}{\partial x^2}}_{\substack{\text{conductive heat transfer} \\ \text{in the direction of the flow}}} - \underbrace{h_{T,air} w_{m,e} (T_{m,air} - T_{air})}_{\substack{\text{convective heat transfer} \\ \text{with the air}}} \\
 & - \underbrace{K_m w_{m,e} (T_{m,air} - T_{m,sol})}_{\substack{\text{conductive heat transfer} \\ \text{between the two sides of the} \\ \text{membrane}}} = 0
 \end{aligned} \tag{14}$$

$$\begin{aligned}
 & \underbrace{k_m \frac{A_m}{2} \frac{\partial^2 T_{m,sol}}{\partial x^2}}_{\substack{\text{conductive heat transfer} \\ \text{in the direction of the flow}}} - \underbrace{h_{T,sol} w_{m,e} (T_{m,sol} - T_{sol})}_{\substack{\text{convective heat transfer} \\ \text{with the solution}}} - \underbrace{K_m w_{m,e} (T_{m,sol} - T_{m,air})}_{\substack{\text{conductive heat transfer} \\ \text{between the two sides of the} \\ \text{membrane}}} \\
 & = 0
 \end{aligned} \tag{15}$$

where k_m (W/m·K), A_m (m²) and K_m (W/m·K) are respectively the thermal conductivity of the membrane, the cross-section area of the membrane and the transversal thermal conductance of membrane per unit length.

4. Regeneration strategy

To regenerate the desiccant solution, an open packed bed system is used. This type of vapor-liquid contact devices is known for its high mass transfer efficiency in a liquid desiccant system (Chung, 1994). In this study, a hot desiccant with a counter-flow configuration was considered due to its higher performance compared to other configurations (liu et al., 2009). The low concentration liquid desiccant entered the

regenerator where counter flow ambient air absorbed the moisture extracted by the desiccant solution in the two membrane sub-systems. The design liquid / air superficial velocity ratio was adjusted in order to obtain a minimum of 50 °C regeneration temperature to assure effective regeneration (Ghaddar et al., 2003).

The regeneration temperature and the outlet enthalpy of the solution were determined by using the general formulas of humidity and enthalpy effectiveness as follow:

$$\varepsilon_y = \frac{W_{air,in} - W_{air,out}}{W_{air,in} - W_{air,eq}} \quad (11)$$

$$\varepsilon_H = \frac{H_{air,in} - H_{air,out}}{H_{air,in} - H_{air,eq}} \quad (12)$$

where ε_y is the humidity efficiency of the regenerator, $W_{air,in}$ (kg of H₂O/kg of dry air) is the humidity ratio of the air at the inlet of the packed bed, $W_{air,out}$ (kg of H₂O/kg of dry air) is the humidity ratio of the air at the exit of the packed bed and $W_{air,eq}$ (kg of H₂O/kg of dry air) is the equilibrium humidity ratio. $H_{air,in}$ (kJ/kg) is the enthalpy of the air at the inlet of the packed bed, $H_{air,out}$ (kJ/kg) is the enthalpy of the air at the exit of the packed bed and $H_{air,eq}$ (kJ/kg) is the equilibrium enthalpy. ε_y and ε_H , and the humidity and enthalpy efficiencies of the regenerator are calculated using the correlations of Martin et al. (Martin and Goswami, 2000).

5. Integration of space and system models and numerical simulation method

In order to compute the conditions inside the indoor space, conditions of the DV supply air are required. They depended on the properties of the membrane exchanger and the conditions of the solution exiting from the space. For this reason, the membrane desiccant boundary layer model, the heat and mass exchanger model, the space model and the regenerator model were coupled. After ensuring comfortable conditions and humidity control, the energy consumption of the cascaded system can be predicted. The input parameters of the integrated model were: 1) space geometry; 2) envelope material; 3) environmental outdoor conditions; 4) liquid desiccant inlet and DV air conditions; 5) The membrane physical properties and geometry of the ceiling membrane system as shown in the flow chart of **Fig. 5**.

The integrated model was simulated by developing a code implemented in MATLAB while assuming all the conditions (temperatures, humidity, concentrations) in the three sub-models to allow the simulation of the space model. The output parameters of the space model were then used to simulate the liquid membrane at the ceiling model to obtain the temperature and concentration of the solution exiting from the space. The membrane exchanger model updated the assumed DV supply air conditions at each iteration. The process of updating the conditions continued until convergence where the relative errors did not exceed 10^{-6} . Once convergence reached, the temperature and humidity in the space were determined. Then, the performance of the cascaded system was assessed through the determination of stratification height and Predicted Mean Vote (PMV). Prediction of the stratification height is of great importance for the assessment of air quality in the occupied zone since it represented the height at which circulating

mass of air became negligible. On the other hand, data acquired from the occupied zone was used to compute the Predicted Mean Vote (PMV) index value using Fanger's expression (Fanger, 1982). In fact, PMV indicates the thermal comfort and satisfaction of the occupants by relating the average temperature, the humidity in the occupied zone, the metabolic rate of occupants and their type of clothing (Fanger, 1982).

Finally, the regenerator model calculated the output temperature of the solution in order to determine the energy required for cooling it before reentering the space. The thermal energy consumption of the system was calculated by taking into account the energy needed to cool the desiccant solution before entering to the space and the energy needed to heat the desiccant solution in the regeneration section.

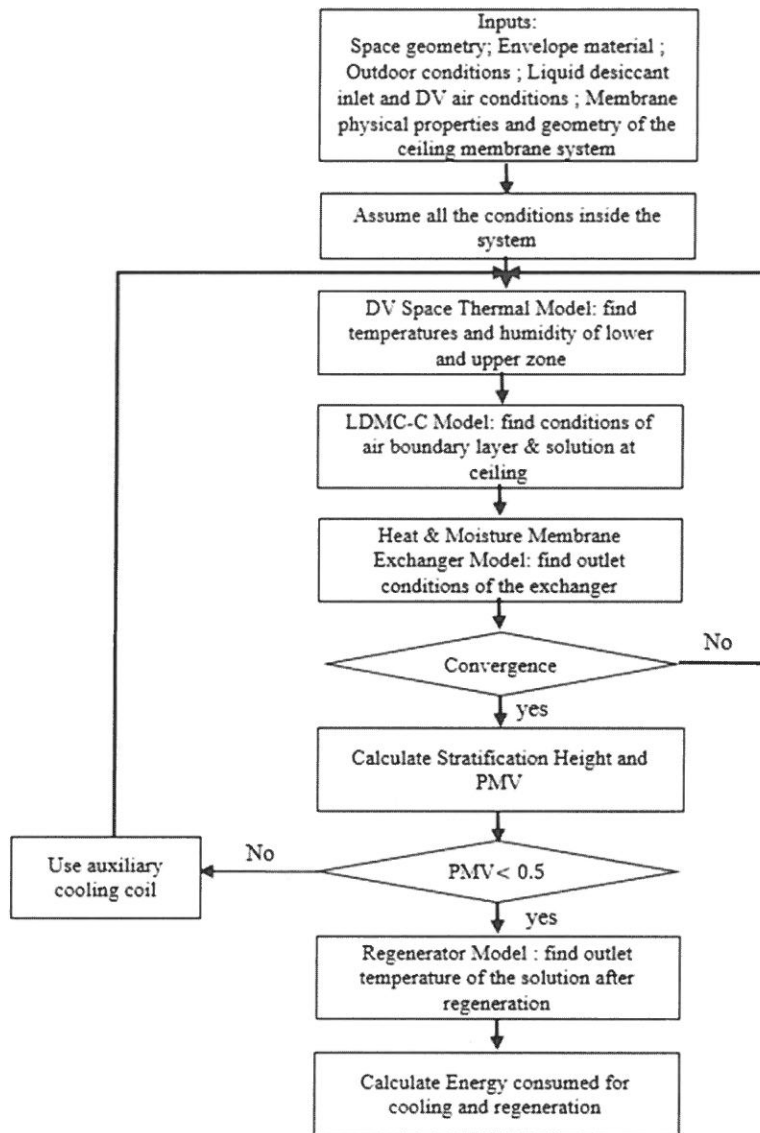


Fig. 5: Sequence of the numerical solution flow chart

B. Experimental Methodology

The objective of the experiments in this study was to validate the integrated transient mathematical model of the cascaded system. The experimentally measured parameters were compared to the theoretical model predictions.

1. *Experimental set up*

Fig. 6 illustrates the schematic of the open circuit experimental set up. The chamber had a floor area of 1 m^2 and a height of 1 m, where the wooden walls were insulated using foam boards to limit the external effects and the internal walls were covered with impermeable sheets to prevent moisture absorption. The membrane cooled ceiling system installed inside the chamber consisted of four baffled membrane panels fabricated following the same experimental procedure adopted by Hout et al. (2017). Each panel had an area of $22 \text{ cm} \times 88 \text{ cm}$ so that the four panels covered about 70% of the ceiling area of the chamber. On the other hand, the outdoor membrane exchanger consisted of 6 membrane plates $20 \times 60 \text{ cm}$ area that separates the adjacent flows of the desiccant solution and air with channel widths of 2 cm and 1 cm respectively. The airside outlets of the exchanger are connected to a supply grill having an area of $25 \text{ cm} \times 25 \text{ cm}$ near the floor of the chamber.

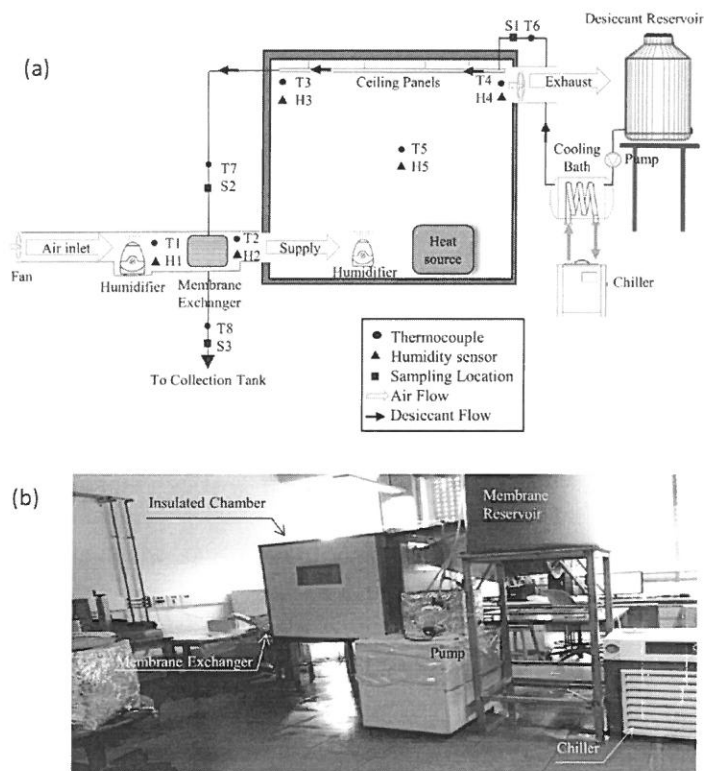


Fig. 6: (a) Illustration of the experimental setup and (b) Photo of the experimental setup

The membrane material chosen for both membrane subsystems was micro porous polypropylene from Sterlitech (Kent, WA, USA) for which the properties are: thermal conductivity of $0.0608 \text{ W/m}\cdot\text{K}$, porosity of 80% and a thickness of $0.2 \mu\text{m}$ (Hout et al., 2017). This material has successively been used in several applications due to its high water vapor permeability and low liquid solution penetration (Larson, 2006). The desiccant material selected was Calcium Chloride (CaCl_2) known for its dehumidification capacity, low corrosiveness properties and low cost (Al-Farayedhi., 2005). The volume of the calcium chloride prepared was 100 liters with a concentration of 37.42 % ($\text{kg CaCl}_2/\text{kg}$ of solution) which is equivalent to $1.6723 \text{ (kg H}_2\text{O/kg CaCl}_2)$.

2. Experimental protocol

The flow of desiccant solution was driven by a small pump and regulated using a globe valve and an analogical flow meter (from Scientific Devises **STVSV with 0.01% accuracy**). The solution was directed to a cooling bath in order to reach the desired temperature. A chiller provided continuous stream of cold water to the cooling bath to assure stable inlet desiccant temperature. The cooled solution flowed through the ceiling panels and the exchanger to finally reach the collector tank. The sizes of the solution reservoir and the collection tank were selected to assure a continuous flow of desiccant for more than 1.5 hours. As for the air, it was supplied to the exchanger using a Honeywell BH-860E humidifier. A suction fan with variable speed was placed at the exhaust grill to provide air flow. The air velocity at exhaust was measured using a BK Precision 731A anemometer with an accuracy of $\pm 3\%$ of full-scale velocity measurement.

In this experimental set up, the real-time measured parameters were (i) the temperature of the air; (ii) the temperature of the solution; (iii) the relative humidity of the air; and (iv) the concentration of the solution. The first two parameters were measured using K-type thermocouples from OMEGA with 0.01 °C accuracy. Relative humidity was measured using relative humidity sensors from OMEGA HX94A series with 0.025 accuracy. The solution mass concentration of the solution was measured by taking samples and analyzing them using a density meter with direct concentration display bought from Anton Paar (DMA4500M) with 0.01 % accuracy. As shown in **Fig. 6**, the thermocouples measuring the air temperature were implemented at the inlet and outlet of the membrane exchanger (T1 and T2), at the beginning of the panel (T3), near

the exhaust grill (T4) and in the middle of the chamber (T5). On the other hand, the thermocouples measuring the solution temperature were implemented at the inlet of the panels (T6), the outlet of the panels (T7) and the outlet of the exchanger (T8). Relative humidity was measured in the following locations: the inlet and outlet of the membrane exchanger (H1 and H2), at the beginning of the panel (H3), near the exhaust grill (H4) and at the middle of the chamber (H5). In addition, samples of solution were taken every 10 min to measure its concentration at the inlet of the panel, the outlet of the panels and at the outlet of the exchanger.

Three cases with different inlet conditions were conducted as presented in **Table 1** to evaluate the reliability of the integrated model in different situations. In the three cases, the air flow rate, the desiccant flow rate, the air humidity ratio and the internal sensible heat generation were kept constant due to their dependency on the equipment' capacities. Moreover, the temperature of the air introduced to the system was at the same ambient temperature of the laboratory where the experiments were conducted. Thus, the inlet parameters that have been changed were the inlet temperature of the solution and the internal moisture generation. The solution inlet temperature in Case 2 was set higher than the other experiments by increasing the set point of the chiller. On the other hand, the internal humidifier was tuned on in Case 3 in order to create an internal moisture generation source. The chiller, the exhaust fan, the pump and the humidifiers were turned on for 1.5 hours in each experiment and the steady-state conditions were reached after 15 to 20 minutes.

Table 1 : Different inlet conditions for the three cases

Parameter	Case 1	Case 2	Case 3
Air Flow rate (L/s)	15±0.24	15±0.24	15±0.24
Desiccant Flow rate (mL/s)	15.7±0.34	15.7±0.34	15.7±0.34
Air inlet Temperature (°C)	23.5 ± 0.4	24.2±0.3	23.7±0.33
Air inlet humidity ratio (g/kg)	14.7± 0.61	14.7± 0.52	14.7±0.56
Solution Inlet Temperature (°C)	12 ± 0.2	16± 0.18	12±0.3
Internal sensible heat (W)	100	100	100
Internal moisture generation rate (g H ₂ O/hr)	0	0	50.3

CHAPTER III

RESULTS AND DISCUSSION

In this section, the results of the experimental validation of the integrated mathematical model are represented. In addition, a case study in which the proposed control strategy was applied to an office space cooled by the LDMC-C/DV system in the hot humid climate of Beirut to study the humidity and energy performance of the system and compare performance with different configurations of the system for humidity control.

A. Experimental validation

In order to validate the mathematical model of the liquid desiccant system, the system was simulated for the physical and geometrical parameters of the experiments. The inlet conditions of the solution and the air measured experimentally were used as inputs for the model to predict the outlet conditions. The measurements and simulation results are shown in **Table 2**.

For the three cases, the maximum relative error in predicting the temperature of the air was 5.3% and the maximum error in predicting the air humidity ratio was 6.1%. As for the desiccant solution, the maximum relative error in predicting the temperature was 6.5%. Furthermore, comparing the values of concentration measurements with the predicted values showed good agreement between the experiment and the mathematical model with a maximum relative error of 0.03%.

Table 2 : Experimental and simulation results for different cases

Parameter		Case 1	Case 2	Case 3
		Inlet Solution T =12 °C no internal moisture	Inlet Solution T =16 °C no internal moisture	Inlet solution T =12 °C + internal moisture
Supply Air Temp (°C) (T2)	Experiment	18.3 ± 0.23	21.2 ± 0.42	18.5± 0.13
	Simulation	18.5	21.5	18.8
Supply Air Hum. (g/kg) (H2)	Experiment	11.5 ± 0.32	11.29 ± 0.41	11.6 ± 0.31
	Simulation	11.3	11.0	11.4
Air Temp Middle Room(°C) (T5)	Experiment	20 ± 0.54	23.1 ± 0.16	20.8 ± 0.34
	Simulation	20.1	23.3	21.2
Air Hum. Middle Room (g/kg) (H5)	Experiment	11.5 ± 0.28	11.3 ± 0.36	14.1 ± 0.43
	Simulation	11.2	11.1	13.6
Exhaust Air Temp. (°C) (T4)	Experiment	16.4 ± 0.36	20.7 ± 0.33	17.8 ± 0.27
	Simulation	16.7	20.8	18.1
Exhaust Air Hum. (g/kg) (H4)	Experiment	11.3 ± 0.34	11.2 ± 0.17	13.4 ± 0.35
	Simulation	10.9	10.8	13.1
Solution Temp. at exit of ceiling (°C) (T7)	Experiment	13.8 ± 0.16	19 ± 0.31	15.3 ± 0.24
	Simulation	14.1	18.4	14.8
Concentration sol. out of the ceiling (kg of H ₂ O/ kg CaCl ₂) (S2)	Experiment	1.6721 ± 0.0001	1.6730 ± 0.0001	1.6775 ±0 .0002
	Simulation	1.6723	1.6733	1.6780
Solution Temp. at exit of exchanger (°C) (T8)	Experiment	18.0 ± 0.35	20.8± 0.15	18.3 ± 0.34
	Simulation	18.2	21.3	18.5
Concentration sol. out of the exchanger	Experiment	1.6819 ± 0.0001	1.6823 ± 0.0001	1.6891 ± 0.0002
	Simulation	1.6822	1.6828	1.6896

Parameter (kg of H ₂ O/ kg CaCl ₂) (S3)	Case 1	Case 2	Case 3
	Inlet Solution T =12 °C no internal moisture	Inlet Solution T =16 °C no internal moisture	Inlet solution T =12 °C + internal moisture

B. Applicability of the humidity control strategy to a case study

Different configurations of the LDMC-C/DV systems were applied to a test case of an office space located in the hot and humid climate of Beirut where their performances were compared based on the humidity levels during the cooling season.

These configurations included the following:

- i) *LDMC-C/DV* without dehumidification at supply;
- ii) *LDMC-C/DV* and a membrane exchanger system with the solution cascaded from the *LDMC-C* outlet to the membrane exchanger;
- iii) *LDMC-C/DV* and a membrane exchanger system where each had a separate feed line for the cool strong solution into it.

The energy consumed by the cascaded system was compared to the energy consumed by the separate feed lines and by a *LDMC-C/DV* system with conventional dehumidification at supply.

1. Description of the case study

The case study comprised of an office space having a floor area of $6\text{ m} \times 6\text{ m}$ with 3 m ceiling height located in Beirut, Lebanon. The office is occupied from 7:00 am to 7:00 pm and a maximum number of 7 occupants were considered inside the room. Each occupant generates 75 W of sensible heat and uses a computer producing 65 W of heat power (Hout et al., 2017). The dynamic internal loads in a typical summer day are given in **Fig. 7**. The sensible internal load represented the sensible heat produced by the occupants, electrical equipment and lighting while the internal latent load represented the water vapor produced by the occupants.

Typical hourly ambient data of typical summer are presented in **Table 3**. An hourly control strategy for each proposed system was adopted to respond to the changes in supply ambient conditions and internal loads during the work hours so that comfort is maintained in the occupied zone.

The membrane ceiling panels were assumed to cover 90% of the total ceiling area and the desiccant solution selected was Calcium Chloride (CaCl_2). For the two membrane systems of ceiling and mass exchanger, the selected membrane material was Polypropylene having 0.2 micrometers pore size for which the properties were stated in the experimental set up section. The membrane exchanger was composed of 30 panels having dimensions of $40\text{ cm} \times 40\text{ cm}$ with air and solution sides' gaps of 0.6 mm and 0.3 mm respectively. As for the packed bed regenerator, the length and the width were 1 m and 0.5 m respectively with a packing material ceramic Intalox saddles with 13 mm maximum thickness which result in an average enthalpy effectiveness 0.81 and an

average humidity effectiveness of 0.79 (Ghaar et al., 2003). For the PMV calculations, the metabolic rate was considered 1.2 Met and the clothes insulation was 1 clo. The efficiency of the heat exchangers was assumed to be 0.8 (Keniar et al., 2015).

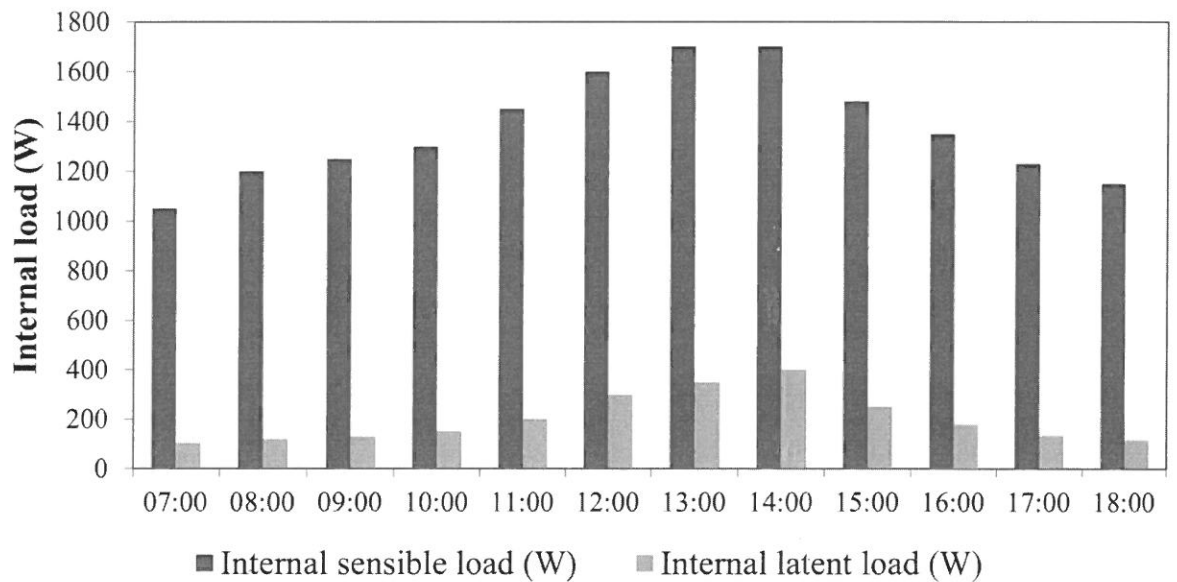


Fig. 7: Internal sensible and latent loads' distributions in the considered office for a typical summer day

Table 3: Ambient Temperature and Relative humidity in four typical days during the summer season in Beirut, Lebanon (Aaboul et al., 2017).

Time	Typical day in June		Typical day in July		Typical day in August		Typical day in September	
	Ambient Temp (°C)	Ambient RH (%)	Ambient Temp (°C)	Ambient RH (%)	Ambient Temp (°C)	Ambient RH (%)	Ambient Temp (°C)	Ambient RH (%)
7:00	25.2	71	25	74	27.4	76	21.8	70

8:00	25.9	71	25.9	69	28.3	72	22.8	69
9:00	26.7	68	26.8	66	29.2	68	23.8	67
10:00	27.4	57	27.6	60	30	64	24.7	62
11:00	28.1	54	28.4	59	30.7	58	25.4	56
12:00	28.6	50	29	56	31.3	56	26.1	55
13:00	28.9	48	29.4	55	31.6	55	26.5	54
14:00	29.1	48	29.7	58	31.8	57	26.8	56
15:00	29	49	29.8	59	31.8	55	26.9	56
16:00	28.7	51	29.7	58	31.6	56	26.8	57
17:00	28.2	54	29.3	60	31.2	59	26.4	61
18:00	27.7	61	28.8	62	30.6	59	25.8	65

2. Performance of the liquid desiccant membrane cooled ceiling combined with displacement ventilation system for the different humidity control strategies

Base case without humidity control (LDMC-C/DV): The indoor space was simulated for the base case where the DV supply air in a *LDMC-C/DV* is only subjected to sensible cooling without any dehumidification. The temperature and the concentration and flow rate of the desiccant solution entering to the ceiling were fixed at 13.5°C, 38% w/w and 0.3 kg/s respectively. The control strategy was based on fixing the temperature of the DV supply air at 20 °C while varying the flow rate of supply air \dot{m}_s to maintain

the temperature in the occupied zone at 23.5°C (± 0.5 °C). The internal loads and ambient conditions are considered for the typical summer days (see Fig.7 and Table 3).

The DV supply flow rates and the resulting occupied zone temperatures of the base case for the cooling season are summarized in Table 4. The relative humidity (RH) in the occupied zone shown in Fig. 8 was a major concern with RH values that ranged from 63.27% to 86.36% in August and elevated RH levels during the summer months. The high humidity values observed would result in many respiratory problems and mold growth and an increasing PMV outside the comfort range. In this case, the air was supplied at low temperature and high ambient humidity ratio which was the reason for the high relative humidity values. Results of the LDMC-C/DV base case established the need for a humidity control strategy based on dehumidifying DV supply air.

Table 4 : Results of base LDMC-C/DV case without dehumidification at DV supply.

Time	Typical day in June		Typical day in July		Typical day in August		Typical day in September	
	\dot{m}_s (kg/s)	T in the occupied zone (°C)	\dot{m}_s (kg/s)	T in the occupied zone (°C)	\dot{m}_s (kg/s)	T in the occupied zone (°C)	\dot{m}_s (kg/s)	T in the occupied zone (°C)
07:00	0.061	23.05	0.061	23.05	0.061	23.06	0.059	23.01
08:00	0.100	23.11	0.100	23.10	0.100	23.12	0.098	23.11
09:00	0.111	23.18	0.111	23.17	0.111	23.17	0.110	23.17
10:00	0.118	23.22	0.120	23.24	0.121	23.24	0.118	23.25

Time	Typical day in June		Typical day in July		Typical day in August		Typical day in September	
	\dot{m}_s (kg/s)	T in the occupied zone (°C)	\dot{m}_s (kg/s)	T in the occupied zone (°C)	\dot{m}_s (kg/s)	T in the occupied zone (°C)	\dot{m}_s (kg/s)	T in the occupied zone (°C)
11:00	0.158	23.30	0.160	23.31	0.160	23.33	0.158	23.33
12:00	0.198	23.41	0.201	23.40	0.201	23.42	0.199	23.46
13:00	0.222	23.54	0.225	23.47	0.225	23.53	0.223	23.50
14:00	0.223	23.54	0.226	23.55	0.226	23.57	0.225	23.56
15:00	0.163	23.40	0.166	23.45	0.166	23.46	0.164	23.44
16:00	0.131	23.23	0.135	23.31	0.135	23.31	0.132	23.29
17:00	0.102	23.17	0.105	23.20	0.105	23.20	0.105	23.19
18:00	0.086	23.04	0.086	23.11	0.086	23.12	0.086	23.08

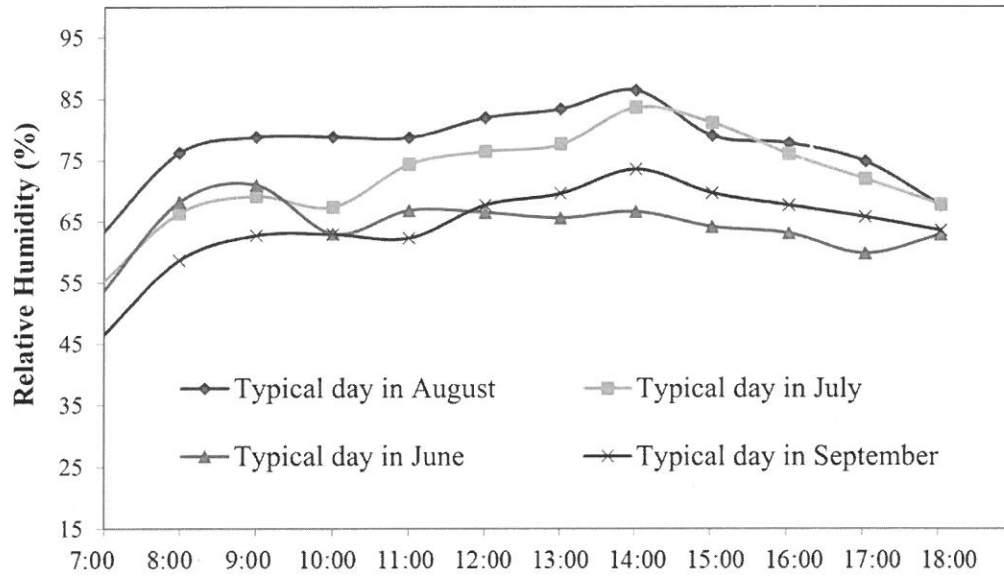


Fig. 8:Relative Humidity in the occupied zone of the considered indoor space for the LDMC-C/DV base case.

Cascaded LDMC-C/DV coupled with a membrane exchanger system: The cascaded system was represented by a LDMC-C/DV system in which the solution exiting from the LDMC-C was cascaded into a membrane exchanger in order to reduce the sensible and latent load of the DV supply air. During the day, the solution entered the ceiling level with fixed inlet temperature (13.5 °C) and concentration (38% w/w) and flow rate (0.3 kg/s) as considered in the base case and the DV supply air \dot{m}_s is considered equal to the air flow rates used in the base case. The system and room were simulated for the same typical days used in the base case (Fig. 7 and Table 3). The proposed control strategy in the cascaded system was based on varying the flow rate of solution cascaded into the exchanger \dot{m}_{sol-ex} so as to deliver ambient fresh air at conditions that meet the hourly dynamic load removal requirements and keep the occupied zone temperature at 23.5 °C (± 0.5 °C). Results of the cascaded system of temperature in the occupied zone and

solution flow rate are summarized in **Table 5** while relative humidity variation is shown in **Fig. 9**.

It can be observed that upon applying the cascaded system with humidity control of the DV supply air, the relative humidity in the occupied zone noticeably decreased compared to the base case. The relative humidity in the occupied zone in August ranged between 39.14% and 71.63%. As for the stratification height in the room, it was greater than the minimum acceptable stratification height to ensure that the clean fresh air is above the breathing level of a seated man (ASHRAE, 2009). In addition, PMV values ranged between 0.21 and 0.47 which represent an acceptable level of thermal comfort. Therefore, applying the cascaded system in a hot and humid day in an office having high internal heat and moisture generation will result in a noticeable drop in the humidity levels in the occupied zone while ensuring acceptable air quality.

Table 5 : Results of LDMC-C/DV with membrane exchanger cascaded system

Time	Typical day in June		Typical day in July		Typical day in August		Typical day in September	
	\dot{m}_{sol-ex} (kg/s)	T in the occup zone (°C)	\dot{m}_{sol-ex} (kg/s)	T in the occup zone (°C)	\dot{m}_{sol-ex} (kg/s)	T in the occup zone (°C)	\dot{m}_{sol-ex} (kg/s)	T in the occup zone (°C)
07:00	0.041	23.08	0.042	23.04	0.047	23.05	0.037	23.00

Time	Typical day in June		Typical day in July		Typical day in August		Typical day in September	
	\dot{m}_{sol-ex} (kg/s)	T in the occup zone (°C)	\dot{m}_{sol-ex} (kg/s)	T in the occup zone (°C)	\dot{m}_{sol-ex} (kg/s)	T in the occup zone (°C)	\dot{m}_{sol-ex} (kg/s)	T in the occup zone (°C)
08:00	0.065	23.11	0.062	23.17	0.074	23.08	0.055	23.09
09:00	0.074	23.16	0.069	23.34	0.085	23.12	0.063	23.17
10:00	0.073	23.21	0.075	23.40	0.097	23.16	0.069	23.18
11:00	0.099	23.33	0.109	23.44	0.143	23.18	0.088	23.21
12:00	0.132	23.36	0.150	23.46	0.220	23.25	0.120	23.29
13:00	0.155	23.43	0.185	23.52	0.275	23.54	0.140	23.42
14:00	0.149	23.61	0.199	23.58	0.285	23.58	0.145	23.51
15:00	0.105	23.38	0.130	23.49	0.150	23.43	0.100	23.49
16:00	0.082	23.27	0.095	23.45	0.110	23.34	0.080	23.41
17:00	0.065	23.18	0.075	23.19	0.079	23.23	0.065	23.26
18:00	0.058	23.05	0.061	23.11	0.072	23.16	0.055	23.13

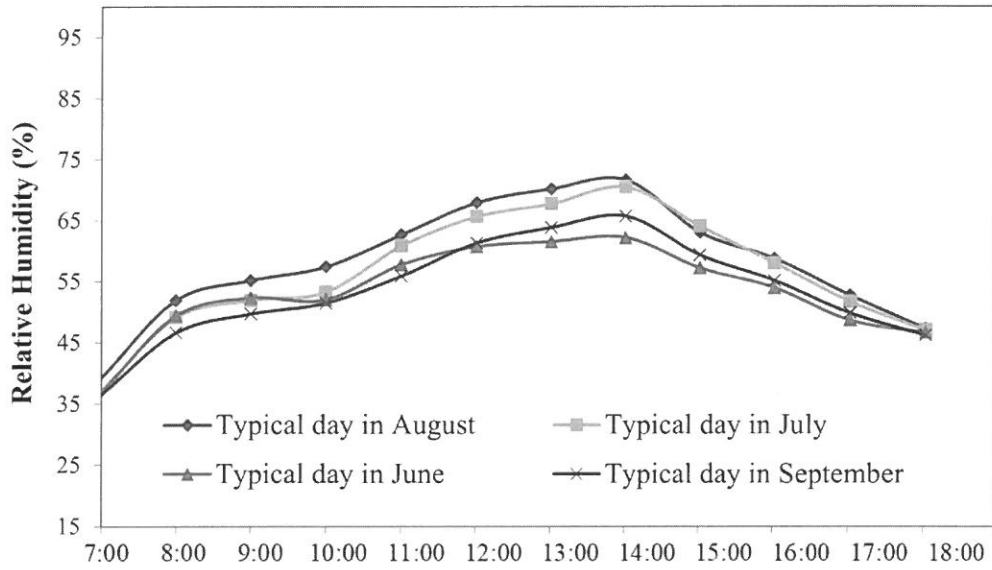


Fig. 9: Relative Humidity in the occupied zone of the considered indoor space for the LDMC-C/DV cascaded system.

Separate feed lines LDMC-C/DV and membrane exchanger system: In order to assure the feasibility of the cascaded system, it was compared to a *LDMC-C/DV* coupled with a membrane exchanger system with separate feed lines to the CC and the membrane exchanger. The cooled and strong liquid desiccant stream was directly supplied to the ceiling and the exchanger at the fixed temperature (13.5°C), concentration (0.38 w/w) and flow rate (0.3 kg/s). As for the air, the flow rate at each hour was considered equal to the flow rate of the supply air in the cascaded system and the base case (see **Table 4**). The hourly control strategy was based on varying the flow rate of the solution entering to the exchanger \dot{m}_{sol-ex} to keep the temperature in the occupied zone at 23.5°C ($\pm 0.5^{\circ}\text{C}$).

Table 6 represents the results of the separate feed line configuration for occupied zone temperature and solution flow rate while **Fig. 10** shows the hourly variation of the relative humidity for each representative day of the summer months. Results showed

that when the separated feed lines system was applied to the room, humidity levels dropped compared to the base case to reach a maximum of 68.55% in August at 14:00. The PMV values in the separated feed lines configuration ranged between 0.19 and 0.46. The comparison of the humidity values between the cascaded and the separate feed lines systems showed that the humidity in the occupied zone was lower by 1.1% to 1.6% in the separate feed line configuration. In addition, in order to obtain nearly equal temperature values in the occupied zone, the separate feed lines system needed less solution flow rate in the exchanger (\dot{m}_{sol-ex}). This was due to the fact that in this system the solution was introduced to the membrane exchanger directly after the cooling stage at a lower temperature and a higher concentration compared to the cascaded system.

Table 3 : Results of LDMC-C/DV in the separate feed lines configuration

Time	Typical day in June		Typical day in July		Typical day in August		Typical day in September	
	\dot{m}_{sol-ex} (kg/s)	T in the occupied zone (°C)	\dot{m}_{sol-ex} (kg/s)	T in the occupied zone (°C)	\dot{m}_{sol-ex} (kg/s)	T in the occupied zone (°C)	\dot{m}_{sol-ex} (kg/s)	T in the occupied zone (°C)
07:00	0.035	23.02	0.035	23.13	0.041	23.03	0.030	23.07
08:00	0.057	23.20	0.056	23.14	0.066	23.07	0.048	23.15
09:00	0.069	23.24	0.068	23.19	0.078	23.19	0.060	23.16

Time	Typical day in June		Typical day in July		Typical day in August		Typical day in September	
	\dot{m}_{sol-ex} (kg/s)	T in the occupied zone (°C)	\dot{m}_{sol-ex} (kg/s)	T in the occupied zone (°C)	\dot{m}_{sol-ex} (kg/s)	T in the occupied zone (°C)	\dot{m}_{sol-ex} (kg/s)	T in the occupied zone (°C)
10:00	0.064	23.28	0.069	23.24	0.084	23.22	0.061	23.22
11:00	0.090	23.32	0.102	23.25	0.120	23.29	0.078	23.30
12:00	0.121	23.34	0.140	23.31	0.178	23.32	0.110	23.35
13:00	0.140	23.40	0.165	23.36	0.224	23.40	0.130	23.38
14:00	0.137	23.46	0.173	23.49	0.230	23.44	0.133	23.42
15:00	0.100	23.40	0.124	23.41	0.136	23.41	0.099	23.39
16:00	0.011	23.37	0.090	23.34	0.095	23.36	0.072	23.34
17:00	0.056	23.33	0.066	23.27	0.070	23.23	0.057	23.34
18:00	0.050	23.20	0.054	23.14	0.051	23.18	0.048	23.20

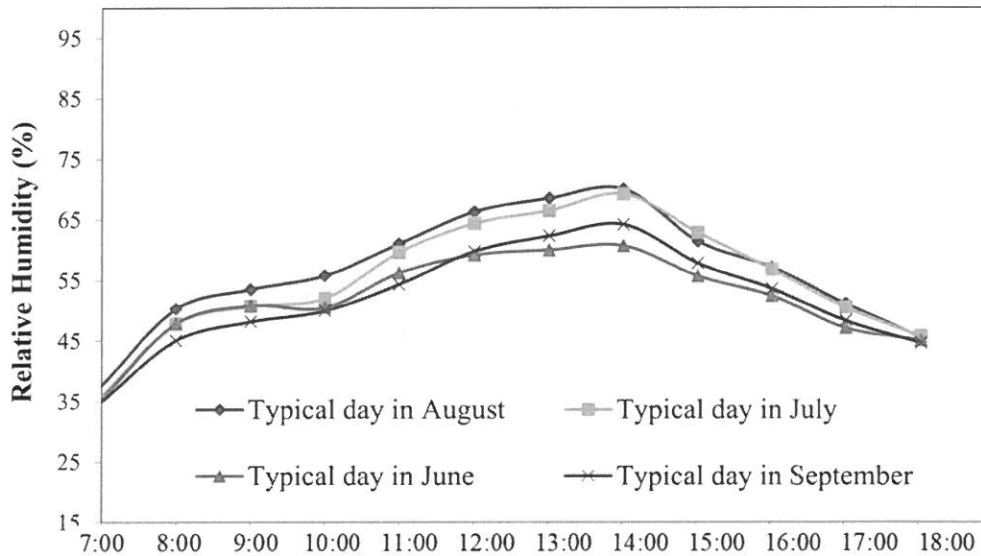


Fig. 10: Relative Humidity in the occupied zone of the considered indoor space for the LDMC-C/DV and membrane exchanger with separate feedlines.

3. Energy Analysis

In this section, the energy consumptions of the different *LDMC-C/DV* with humidity control strategy systems were computed and analyzed. These systems included the *LDMC-C/DV* cascaded system, the *LDMC-C/DV* separate feed line system and the *LDMC-C/DV* with conventional dehumidification at supply. The energy consumptions of the two first systems were computed for the cooling season from the thermal energy needed to cool the strong desiccant solution in addition to the energy needed to heat the desiccant solution for regeneration. In the cascaded configuration, a fraction of the solution exiting from the ceiling was cascaded into the heat exchanger. Then, the desiccant solution exiting from the exchanger was mixed with the remaining fraction of the solution exiting from the ceiling to be directed to the heating and regeneration section. For the separate feed lines configuration, each membrane subsystem was

directly supplied with cooled and strong desiccant solution. Then, the two flows exiting from the membrane subsystems were mixed and directed to the heating and regeneration section. In order to reduce the heating energy consumption, a liquid-liquid heat exchanger was implemented between the inlet and outlet of the heating and regeneration section. An air-air heat exchanger was also implemented between the ambient inlet air and the exhaust air to reduce the cooling energy consumed. For the *LDMC-C/DV* the system with conventional dehumidification, a Subcool- Reheat method was used, where the ambient air was cooled until it has a humidity ratio equal to the humidity ratio of the air supplied in the cascaded system. Then, the air was reheated to reach the temperature of the supply air in the cascaded system.

Fig. 11 and **Fig. 12** show the monthly heating and cooling energy consumption respectively for the liquid desiccant systems in the cooling season. Results of the three systems showed that when the average relative humidity in a month increased, the energy consumption in a *LDMC-C/DV* system increased. This observation is essentially related to the fact that any increase in the ambient relative humidity increases the moisture removed by the two membrane sub-systems which increases the regeneration temperature. The cooling and heating energy consumptions were higher in the separate feed lines configuration than in the cascaded configuration. In August the cooling energy in the cascaded configuration was lower by 21.25 % than in the separate feed lines configuration and the heating energy was lower by 16.23%. In the separate lines system, the solution was introduced to the exchanger and the ceiling at the same low desiccant temperature introduced to the cascaded system but with higher total flow rate which resulted in higher heating and cooling energy consumption. In addition, the

cooling energy consumption in the cascaded system was lower by 23.19% than the cooling energy in the system with conventional dehumidification and the heating energy was lower by 21.13%.

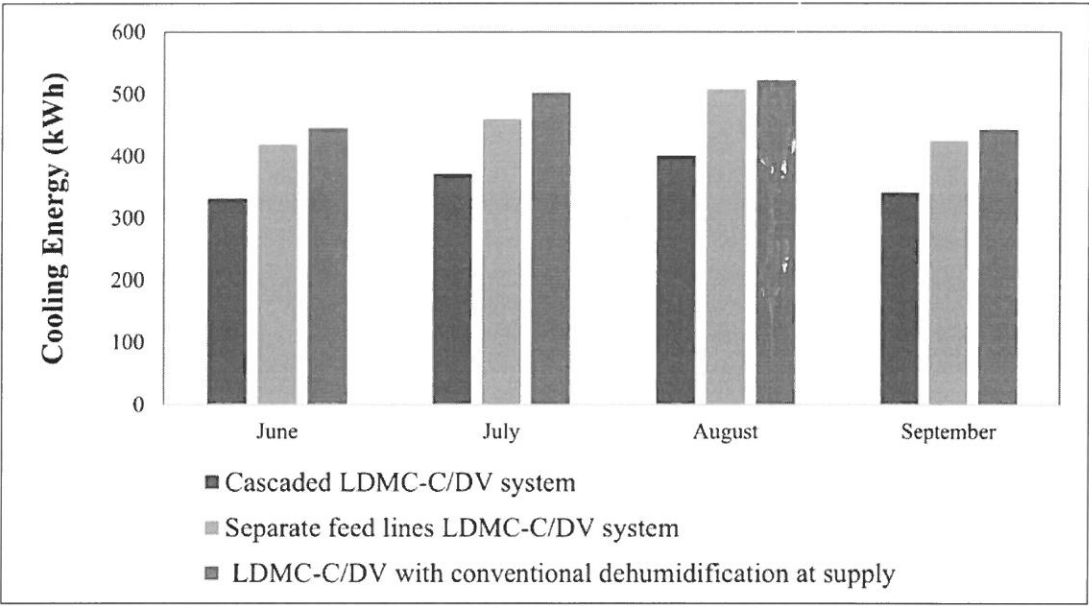


Fig. 11: Monthly cooling energy consumption of the different LDMC-C/DV configurations for humidity control

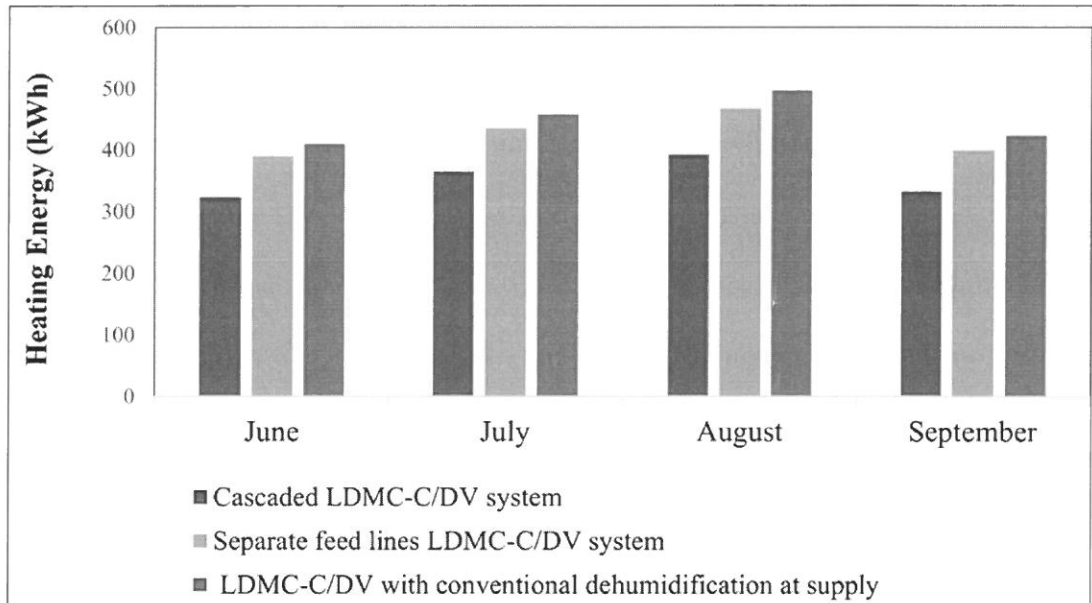


Fig. 12: Monthly heating energy consumption of the different LDMC-C/DV configurations for humidity control

C. Conclusions

The performance of a cascaded liquid desiccant system in a hot and humid climate has been studied using a validated mathematical model. The cascaded system is based on directing the solution exiting from a membrane CC system to a membrane exchanger located at the DV supply in order to reduce the sensible and latent heat of the supply air. The performance of the system was assessed in a case study representing an office space located in a hot and humid climate and having high internal moisture generation.

Applying the cascaded system had a noticeable effect on reducing the relative humidity in the occupied zone compared to a *LDMC-C/DV* system without a humidity control strategy. The performance of the cascaded system was also compared to a

LDMC-C/DV and membrane exchanger with separate feed lines configuration. The latter showed slightly lower humidity levels by 1.1 % to 1.6% in the occupied zone compared to the cascaded configuration. However, the cooling and heating energy consumed by the cascaded system during the cooling season was lower by 21.25% and 16.23% respectively in August compared to a *LDMC-C/DV* and membrane exchanger with separate feed lines configuration and by 23.19% and 21.13% compared to *LDMC-C/DV* with conventional humidity control.

BIBLIOGRAPHY

U.S. Environmental Protection Agency, Report to Congress on indoor air quality.

EPA/400/1-89/001C. Washington, DC 1989:2.

Vesely M, Zeiler W. Personalized conditioning and its impact on thermal comfort and energy performance – A review. *Renewable and Sustainable Energy Reviews* 2014; 43: 401-266. doi: 10.1016/j.enbuild.2015.07.055.

Al Assaad D, Ghali K, Ghaddar N, Habchi C. Mixing ventilation coupled with personalized sinusoidal ventilation: optimal frequency and flow rate for acceptable air quality. *Energy and Buildings*, 2017; 154: 569-580. doi: 10.1016/j.enbuild.2017.08.090.

Itani M, Ghali K, Ghaddar N. Increasing energy efficiency of displacement ventilation integrated with an evaporative-cooled ceiling for operation in hot humid climate. *Energy and Buildings* 2015; 105: 26-36. 10.1016/j.enbuild.2015.07.055

- Chua K J, Chou S K, Yang WM, Yan J. Achieving better energy-efficient air conditioning—a review of technologies and strategies. *Applied Energy* 2013; 104: 87-104. [10.1016/j.apenergy.2012.10.037](https://doi.org/10.1016/j.apenergy.2012.10.037)
- Ghaddar N, Ghali K, Saadeh R. Optimized selection and operation of the combined chilled ceiling system and displacement ventilation. *International Journal of Energy Research* 2010;34: 1328–40. doi: [10.1002/er.1677](https://doi.org/10.1002/er.1677). doi: [10.1002/er.1677](https://doi.org/10.1002/er.1677)
- Yuan X, Chen Q, Gliksman, LR. A critical review of displacement ventilation, *ASHRAE Trans* 1998; 104: 78-90
- Mossolly M, Ghaddar N, Ghali K. Optimized operation of combined chilled ceiling displacement ventilation system using genetic algorithm. *ASHRAE Trans* 2008; 143: 541-554
- Hao X, Zhang G, Chen Y, Zou S, Moschandreas, D. J. A combined system of chilled ceiling, displacement ventilation and desiccant dehumidification. *Building and Environment* 2007; 42(9): 3298-3308. doi:[10.1016/j.buildenv.2006.08.020](https://doi.org/10.1016/j.buildenv.2006.08.020)
- Younis M, Ghali K, Ghaddar N. Performance evaluation of the displacement ventilation combined with evaporative cooled ceiling for a typical office in Beirut. *Energy Conversion and Management* 2015; 105:655-664. doi: [10.1016/j.enconman.2015.08.030](https://doi.org/10.1016/j.enconman.2015.08.030).
- Yin Y, Wang R, Zhai X, Ishugah T. Experimental investigation on the heat transfer

- performance and water condensation phenomenon of radiant cooling panels. *Building and Environment* 2014; 71: 15–23. doi: 10.1016/j.buildenv.2013.09.016
- Keblawi, A., Ghaddar, N., & Ghali, K. (2011). Model-based optimal supervisory control of chilled ceiling displacement ventilation system. *Energy and Buildings* 2011; 43(6): 1359-1370. doi:10.1016/j.enbuild.2011.01.021.
- Fauchoux M, Simonson CJ, Torvi DA. Tests of a Novel Ceiling Panel for Maintaining Space Relative Humidity by Moisture Transfer from an Aqueous Salt Solution. *ASTM International* 2009;6:1-10. doi: 10.1520/JAI102034.
- Hout M, Ghaddar N, Ghali K, Ismail N, Simonetti M, Fracastoro G, Zoughaib A. Displacement ventilation with cooled liquid desiccant dehumidification membrane at ceiling; modeling and design charts. *Energy* 2017; 139;1003:1015. doi: 10.1016/j.energy.2017.08.046
- Keniar K, Ghali K, Ghaddar N. study of solar regenerated membrane desiccant system to control humidity and decrease energy consumption in office spaces. *Applied Energy* 2015;138:121-132. doi: 10.1016/j.apenergy.2014.10.071
- Muslmani M, Ghaddar N, Ghali M. Performance of combined displacement ventilation and cooled ceiling liquid desiccant membrane system in Beirut climate. *Journal of Building Performance Simulation* 2016;9: 648-662. doi: 10.1080/19401493.2016.1185153
- Seblany R, Ghaddar N, Ghali K, Ismail N, Simonetti M, Virgone J, Zoughaib A.

- Humidity control of liquid desiccant membrane ceiling and displacement ventilation system. *Applied Thermal Engineering* 2018; 144: 1-12. doi:10.1016/j.applthermaleng.2018.08.036
- Abdel-Salam AH, Simonson CJ. State-of-the-art in liquid desiccant air conditioning equipment and systems. *Renewable and Sustainable Energy Reviews* 2016; 58: 1152-1183. doi: 10.1016/j.rser.2015.12.042
- Charara J, Ghali K, Ghaddar N, Mustapha R, Assaad Z. Liquid Desiccant Cascaded System for Indoor Air Conditioning. In 10th International Conference on System Simulation in Buildings (SSB 2018).
- Makhoul A, Ghali K, Ghaddar N. The energy saving potential and the associated thermal comfort of displacement ventilation systems assisted by personalized ventilation. *Indoor and Built Environment* 2013; 22(3): 508-519. doi:10.1177/1420326x12443847.
- Al Assaad D, Habchi C, Ghali K, Ghaddar N. Simplified model for thermal comfort, IAQ and energy savings in rooms conditioned by displacement ventilation aided with transient personalized ventilation. *Energy Conversion and Management* 2018; 162: 203-217. doi: 10.1016/j.enconman.2018.02.033
- Ayoub M, Ghaddar N, Ghali k. Simplified Thermal Model of Spaces Cooled with Combined Positive Displacement Ventilation and Chilled Ceiling System. *HVAC&R Research*; Atlanta 2006;12: 1005-1030.
- Schiavon, Stefano, et al. Room air stratification in combined chilled ceiling and displacement ventilation systems. *HVAC&R Research* 18.1-2, 2012: 147-159. doi: 10.1080/10789669.2011.592105

- Mundt E. The performance of displacement ventilation systems: Experimental and theoretical studies, Royal Institute of Technology 1996.
- Jaluria Y. Natural convection: heat and mass transfer. Elkins Park (Pa.): Franklin; 1994.
- Zhang LZ. Total heat recovery: heat and moisture recovery from ventilation air. New York: Nova Science Publishers Inc.; 2008.
- Grossman G. Solar cooling, dehumidification, and air-conditioning. Encyclopedia of Energy 2004: 575–585.
- Abdel-Salam AH, Ge G, Simonson C. Performance analysis of a membrane liquid desiccant air-conditioning system. Energy and Buildings 2013;62: 559-569. doi: 10.1016/j.enbuild.2013.03.028
- Mustapha R, El Khoury K, Assaad Z. A Hybrid no Frost Refrigeration System Using a Membrane Based Desiccant System. In 30th International Conference on Efficiency, Cost, Optimization, Simulation and Environmental Impact of Energy Systems (ECOS 2017), 2 to 6 July 2017, San Diego State University, San Diego, USA.
- Chung T W. Predictions of moisture removal efficiencies for packed-bed dehumidification systems. Gas separation & purification 1994; 8(4): 265-268. doi: 10.1016/0950-4214(94)80007-3
- Liu X H, Jiang Y, Yi XQ. Effect of regeneration mode on the performance of liquid desiccant packed bed regenerator. Renewable Energy 2009; 34(1): 209-216. doi: 10.1016/j.renene.2008.03.003
- Ghaddar N, Ghali K, & Najm A (2003). Use of desiccant dehumidification to improve

- energy utilization in air-conditioning systems in Beirut. *International Journal of Energy Research* 2003; 27(15): 1317-1338. doi: 10.1002/er.945
- Martin V, Goswami DY. Effectiveness of Heat and Mass Transfer Processes in a Packed Bed Liquid Desiccant Dehumidifier/Regenerator. *HVAC&R Research* 2000; 6(1): 21-39. doi:10.1080/10789669.2000.10391248
- Fanger PO. *Thermal Comfort Analysis and Applications in Engineering*. New York: McGraw Hill, 1982.
- Larson, M. D. The performance of membranes in a newly proposed runaround heat and moisture exchanger. University of Saskatchewan Saskatoon; 2006
- Al-Farayedhi AA, Gandhidasan P, Antar MA, Gaffar MS. Experimental study of an aqueous desiccant mixture system: Air dehumidification and desiccant regeneration. *Proceedings of the Institution of Mechanical Engineers, Part A: Journal of Power and Energy* 2005; 219(8): 669-680. doi:10.1243/095765005x69233
- Daaboul J, Ghali K, Ghaddar N. Mixed-mode ventilation and air conditioning as alternative for energy savings: A case study in Beirut current and future climate. *Energy Efficiency* 2017;11(1): 13-30. doi:10.1007/s12053-017-9546-z
- Jentsch, MF, Bahaj AS, James PA. Climate change future proofing of buildings Generation and assessment of building simulation weather files. *Energy and Buildings* 2008;40(12):2148-2168.
- ASHRAE Handbook -Fundamentals. 2009. American Society of Heating Refrigerating and Air-Conditioning Engineers. Chapter 9. Atlanta, USA.

